Stimulated rotational and vibrational Raman scattering by elliptical polarized pump radiation

F. De Tomasi, D. Diso, M. R. Perrone,* and M. L. Protopapa

Dipartimento di Fisica, INFM, Instituto Nazionale di Fisica della Materia, Universita' di Lecce, 73100 Lecce, Italy
(Received 11 August 2000; revised manuscript received 20 March 2001; published 13 July 2001)

Stimulated rotational and vibrational Raman scattering is investigated with a XeCl excimer laser by varying either the ellipticity degree of the pump radiation polarization and the pump beam quality factor (M^2) and divergence (θ). It is shown that the dependence of stimulated rotational Raman scattering upon pump radiation polarization is substantially influenced by the optical properties (M^2 and θ) of the pump beam. Gain suppression effects on stimulated vibrational Raman scattering and their dependence on pump beam optical properties have been evaluated to support experimental results. Introducing the effective vibrational Raman gain provides a good understanding of the experimental results.

I. INTRODUCTION

Stimulated Raman scattering [1] in gases may occur for both stimulated vibrational Raman scattering (SVRS) and stimulated rotational Raman scattering (SRRS) transitions and has been widely used as a method of generating tuneable radiation. A large amount of research has mainly been devoted to SVRS since the threshold is generally more easily reached, SRRS being more difficult to observe [2]. At high pressures, vibrational Raman scattering, for whom the threshold falls with rising pressure, suppresses SRRS, whereas the threshold for rotational scattering is not pressure dependent above one bar. Moreover, rotational energy levels are degenerate in angular momentum, and therefore, the scattering is sensitive to pump polarization and circularly polarized pump beams are generally used to eliminate Stokes-anti-Stokes interactions and observe SRRS. The SVRS gain is polarization independent.

A growing interest toward SRRS has been observed in the last years [3–7] in view of extending the tuning range of several laser sources. Single-pass conversion efficiencies to the first rotational Stokes as high as 80% have been reported in [7] by pumping H_2 with a Q switched, frequency doubled Nd-YAG laser. Nevertheless, few theoretical treatments and still less experimental verification have been reported on SRRS, and the conditions that favor the Raman conversion to rotational lines with respect to vibrational lines are still not well defined. We have recently reported [8,9] on SRRS in H_2 pumped by XeCl excimer lasers to investigate the dependence of rotational scattering on pump polarization and focusing geometry. It was shown in [8] that, with a circularly polarized pump beam, a high-angle focusing geometry allows us to get only rotational Raman scattering, whereas a low-angle focusing geometry provides only vibrational Raman scattering for gain suppression effects. Moreover, it was shown in [9] that the dependence of SRRS on pump radiation polarization is affected by the focusing geometry, i.e., whether low- or high-angle focusing is applied. Experimental results were in accordance with theory mainly at high-

angle focusing geometries and it was shown that gain suppression effects on SVRS have to be considered in understanding the experimental results.

Further experimental investigations are reported in this paper to gain a better understanding of theory. In particular, SRRS has been investigated by varying the optical properties of the pump radiation and the ellipticity degree of the pump radiation polarization. SRRS is sensitive to the pump radiation polarization, whereas gain suppression on SVRS is affected by the diffraction angle propagating within the pump focal zone that depends on the pump beam optical properties. When a pump beam is focused in the Raman medium, gain is expected to be suppressed if the phase-matched angles of the Stokes and anti-Stokes waves are well contained within the diffraction angle occurring in the pump focal zone.

This systematic study may provide a better knowledge of the main conditions favoring rotational scattering with respect to vibrational scattering when high-power, broadband, multimode laser beams are focused in a Raman medium. Information taken both from the literature and in the course of our work has been collected to provide a good understanding of theory and experiments. The main points of the theory on vibrational and rotational Raman scattering are reviewed in Sec. II. Experimental details and results are given in Sec. III. Discussion and conclusion are reported in Sec. IV.

II. THEORY

A detailed account of the steady-state theory of stimulated vibrational Raman scattering has been given in 1965 by Shen and Bloembergen [10]. They showed that the stimulated Raman radiation would grow as a mixed mode containing both Stokes and anti-Stokes components in the presence of Stokes/anti-Stokes coupling. In particular, they have shown that for nonzero values of the linear momentum mismatch Δk in the direction of beam propagation z, the Stokes and anti-Stokes field amplitude have exponential growth of the form $\exp(\Gamma z)$, where the Raman gain coefficient per unit length Γ is given by [11]

$$\Gamma = \mathrm{Re}\{(1/2)(K_3 - K_1)|A_p|^2 - (i/2)[\Delta k^2 + 2i\Delta k(K_3 + K_1)|A_p|^2 - (K_1 - K_3)^2|A_p|^4]^{1/2}\}. \quad (1)$$

*Corresponding author: FAX: +39 0832 320505. Email address: perrone@le.infn.it

A_p is the pump field amplitude; $K_1 = -iK_{AS}\chi_{AS}$ and $K_3 = -iK_S\chi_S^*$, where χ_S and χ_{AS} are the nonlinear susceptibilities for stimulated growth of the Stokes and anti-Stokes waves, respectively; $K_{S(AS)} = 2\pi N\omega_{S(AS)}/(n_{S(AS)}c)$, where N is the number density, $\omega_{S(AS)}$ is the Stokes (anti-Stokes) frequency, and $n_{S(AS)}$ is the linear index of refraction at $\omega_{S(AS)}$.

Equation (1) leads to the quite surprising result that the coupled gain Γ vanishes in the limit of perfect phase matching ($\Delta k = 0$), condition under which the Stokes and anti-Stokes waves grow nonexponentially. Indeed, the growth of the Stokes and anti-Stokes amplitudes A_S and A_{AS}, respectively, is initially linear in z at phase matching. Then, it slows down as z increases until the condition

$$A_S(z) = -(K_1/K_2)A_{AS}(z) \tag{2}$$

is asymptotically approached at large z, in which limit neither the Stokes nor the anti-Stokes wave grows further (gain suppression), where $K_2 = -iK_{AS}(\chi_{AS}\chi_S^*)^{1/2}$.

Experimental evidence of gain suppression effects has taken the form of unexpectedly high thresholds, of dark regions in the Stokes emission, of anti-Stokes emission at angles offset from the phase-matching direction, and of Stokes amplification below theoretical expectations. It is worth noting that the conditions allowing perfect phase matching between pump, Stokes, and anti-Stokes fields and then gain suppression effects are affected by focusing geometry and pump beam optical characteristics. When a pump beam is focused in the Raman medium, gain is expected to be suppressed if the phase-matched angles of Stokes and anti-Stokes waves are well contained within the diffraction angle δ propagating within the pump focal zone. The phase-matched angles of Stokes and anti-Stokes waves may be computed for the simple angle phase-matching diagram of Fig. 1 of [12], and one gets $\varphi_S = 5.15$ mrad and $\varphi_{AS} = 3.98$ mrad for the phase-matched angles of the vibrational Stokes and anti-Stokes wave, respectively, by using published measurements of H_2 refractive indexes [13] and 15 bar of H_2. Whereas, the diffraction angle may be computed by the following relation [8]

$$\delta \cong \lambda_p M^2/(\sqrt{2}\pi f\theta), \tag{3}$$

where f is the focal length of the focusing lens, and M^2 and θ are the beam quality factor and the full-angle divergence of the pump radiation of wavelength λ_p. The optical beam parameters M^2 and θ are linked by the following relation [14]

$$\theta w_p = (2\lambda_p/\pi)M^2, \tag{4}$$

where w_p is the pump beam radius. As it has previously been mentioned, gain on vibrational scattering is expected to be suppressed if $\delta \geq \varphi_S$ and as a consequence, the optical beam parameters M^2 and θ, besides f, affect gain suppression on SVRS.

Let us mention that in absence of anti-Stokes emissions, Eq. (1) provides the steady-state gain per unit length of pure Stokes generation Γ_V that is given by

$$\Gamma_V = \text{Re}[-i(2\pi N\omega_S/n_S c)\chi_s^*|A_p|^2] \tag{5}$$

In the presence of anti-Stokes emission, the Stokes amplification approaches its unsuppressed Γ_V value as the wave-vector mismatch becomes large enough to allow the Stokes and anti-Stokes waves to decouple, and this is predicted to occur when $\Delta k \geq 2\Gamma_V$.

Let us introduce the more commonly used steady-state Raman gain coefficient g_V that for a laser pulse of energy E_p and time width Δt is given by

$$g_V = \Gamma_V(\Delta t/E_p). \tag{6}$$

It can be shown [8] that at H_2 pressures larger than 10 bar and at the XeCl laser wavelength ($\lambda_p = 308$ nm) it takes the value $g_V = 7.6 \times 10^{-9}$ cm/W.

A detailed theoretical account of the influence of the anti-Stokes radiation on the rotational Raman gain coefficient g_R has been given by Venkin, Ilinskii, and Mikheev [15]. Let us mention that the largest gain results from counter rotating circularly polarized beams for pure rotational transitions. As a consequence, the generation of anti-Stokes lines is not expected to occur, since the transfer of angular momentum implies that the four-wave-mixing processes disappear when pump and Stokes photons copropagate and are circularly polarized in opposite senses. However, elliptical polarized pump radiation allows the anti-Stokes line to occur and, as a consequence, gain suppression effects on rotational Stokes are also expected. The wave mismatch is rather small for rotational scattering, as a result of the small frequency shift and then, the perfect phase-matching condition can be easily reached. Following the work of Venkin, Ilinskii, and Mikheev one gets for a zero wave mismatch that the rotational Raman gain coefficient of the S_{01} line is given by

$$g_R = \{\Delta N[8\pi^3 C(J)(\gamma_{\nu,J;\nu,J+2})^2]/[15cn_S\lambda_s h\Delta\nu]\}$$
$$\times(6\sin 2\psi), \tag{7}$$

where

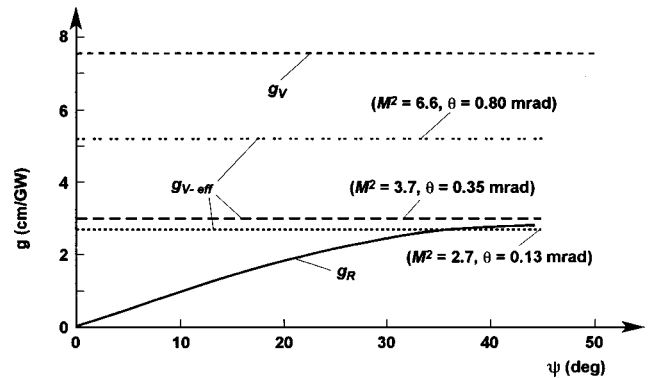$$C(J) = [(J+1)(J+2)]/[(2J+1)(2J+3)]. \tag{8}$$

FIG. 1. Rotational Raman gain g_R versus the ellipticity angle (solid line). The noncontinuous lines represent g_V and different values of the effective vibrational gain $g_{V\text{ eff}}$.
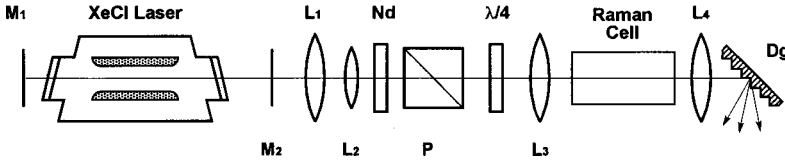
FIG. 2. Layout of the experimental setup.

$\gamma_{\nu,J;\nu,J+2}$ is the off-diagonal element of the molecular anisotropic polarizability; λ_S is the wavelength of the Stokes beam; $\Delta\nu$ is the Raman line width [half width at half maximum (HWHM)]; ΔN is the number density difference between the initial state J and the final state $J'=J+2$; ψ is the ellipticity angle that varies between ± 45 and $0°$, as the pump radiation polarization changes from circular ($|\psi|=45°$) to linear ($|\psi|=0°$). Figure 1 shows g_R (solid line) versus ψ. We have used published data to calculate g_R at 15 bar of H_2. Indeed, we have set the number density difference $\Delta N = 2.1 \times 10^{20}$ cm^{-3}, the linewidth $\Delta\nu = 0.75$ GHz and $(\gamma_{\nu,J;\nu,J+2})^2 = 15.7 \times 10^{-50}$ cm^6 according to [8,16], and [17]. One observes from Fig. 1 that g_R reaches its maximum value of 2.86×10^{-9} cm/W for circularly polarized pump beams ($\psi=45°$) whereas, it reaches a null value for linearly polarized beams ($\psi=0°$). The vibrational Raman gain g_V, which is ψ independent is also shown for comparison on Fig. 1 and one observes that $g_V \cong 2.6g_R$ at $\psi=45°$ and that the ratio g_R/g_V increases with ψ. Hence, the competition between rotational and vibrational scattering is expected to depend upon ψ.

III. EXPERIMENTAL SETUP AND RESULTS

The layout of the experimental apparatus is shown in Fig. 2. A locally made, discharge-excited XeCl laser is used as radiation source. The laser is fitted with unstable cavities to get low-divergence laser radiation as required in SRS studies. Indeed, three different unstable cavities (Fig. 3) are applied to the XeCl laser to get laser beams characterized by different beam quality factor (M^2) and divergence (θ) values. The laser beam with lowest divergence and M^2 parameter is obtained by an unstable cavity (A) of magnification factor $F_M=4.7$ made of an aluminised convex mirror with 100 cm radius of curvature (M_1) and a flat phase-unifying (PU) mirror set 73 cm apart (M_2). The PU mirror is characterized by a high reflectivity ($R_0=0.67$) central spot of 3.5 mm diameter [Fig. 3(a)]. A discussion on the benefits of PU output couplers in unstable cavities is reported in [18]. The largest divergence and M^2 laser beam is delivered by cavity C that is obtained by replacing the PU mirror with a flat quartz [Fig. 3(c)]. The third unstable cavity (B) of magnification factor $F_M=3.65$ is obtained by replacing M_1 with a convex mirror of 150 cm radius of curvature [Fig. 3(b)]. The randomly polarized laser beam with a cross section of about 20 mm $\times$ 10 mm is collimated and demagnified by two lenses L_1 and L_2 and is elliptical polarized by means of a polarizing beam splitter cube P and a $\lambda/4$ plate (Fig. 2). The degree of ellipticity of the pump radiation is varied smoothly between circular ($|\psi|=45°$) and linear ($|\psi|=0°$) by rotating the $\lambda/4$ plate whose optical axis is perpendicular to the incident radiation and then, by changing the ellipticity angle ψ. All laser

beams are focused by a lens of 21-cm focal length (L_3) in a 27-cm long Raman cell filled with H_2 at a total pressure of 15 bar. Full-angle beam divergence θ and beam quality factor values of all tested laser beams are reported on Table I besides the corresponding diffraction angle values computed by Eq. (3). All laser pulses are characterized by a time width $\Delta t = 13$ ns duration (FWHM, full width at half maximum). The XeCl laser spectrum [19] mainly consists of two relatively narrow isolated lines due to the two strongest 0–1 and 0–2 electronic transitions at 3079.9 Å and at 3082.1 Å having a spectral width of 0.4 Å ($\Delta V = 126$ GHz) and of 0.2 Å, respectively. So, SRS is investigated in this work by a multimode pump beam with a bandwidth much larger than the bandwidth of the rotational and vibrational transition [8].

Neutral density filters (Nd) are used to vary pump beam energy E_p. Laser beams at the exit of the gas cell are collimated by the lens L_4 and dispersed by a grating Dg. Pyroelectric detectors are used to sample beam energies and fast photodiodes and a storage oscilloscope are used to monitor pulse evolutions in time. High purity (99,9999%) H_2 is used in all measurements.

Let us present the main experimental results that will be discussed in the following section. Raman conversions to the first rotational Stokes line (S_{01}) of orthohydrogen at 313.7 nm ($\nu=0$, $J=1 \rightarrow \nu=0$, $J=3$), to the first vibrational line S_{10} at 353.2 nm ($\nu=0$, $J=1 \rightarrow \nu=1$, $J=1$), and to S_{11} at 360.7 nm ($\nu=1$, $J=1 \rightarrow \nu=1$, $J=3$) have only been observed. Figure 4 shows the energy conversion efficiencies to Raman radiation as a function of pump beam energy and at
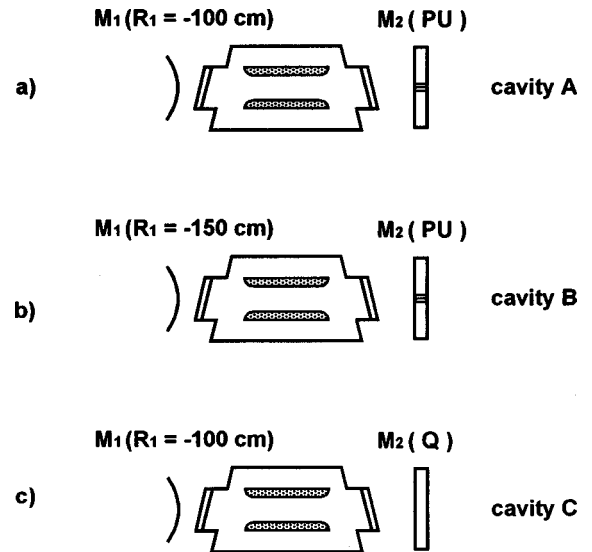

FIG. 3. Layout of the unstable cavities applied to the XeCl laser: PU, phase unifying mirror; Q, quartz window, (a) PU unstable cavity of magnification factor $F_M=4.7$; (b) PU unstable cavity with $F_M=3.65$; (c) conventional unstable cavity with $F_M=4.7$.

TABLE I. Laser beam optical parameters (M^2 and θ), diffraction angle δ, energy threshold for vibrational scattering $E_{V,\text{th}}$ and effective vibrational Raman gain $g_{V\text{-eff}}$.

Cavity	M^2	θ (mrad)	δ (mrad)	$E_{V,\text{th}}$ (mJ)	$g_{V\text{-eff}}$ (cm/GW)
A	2.7	0.13	7.2	3.3	2.7
B	3.7	0.35	6.7	4.2	3.0
C	6.6	0.80	5.4	4.4	5.2

different ψ angles, for the pump beam provided by cavity A, B, and C. The energy conversion efficiencies for circular polarized pump radiation ($|\psi|=45°$) and for the elliptical polarized radiation providing conversion efficiencies to S_{01} of about 1% at the highest pump energies, are reported on Fig. 4. ψ_{th} represents the ellipticity angle at which the energy conversion efficiency to S_{01} reduces to about 1% at the highest pump energies.

The highest conversion efficiencies to S_{01} have been obtained for circular polarized pump radiation under all tested experimental conditions, accordingly to theory [2]. However,

the conversion efficiency to S_{01} reduces as θ and M^2 increase, whereas the conversion to S_{10} increases with θ and M^2. Indeed, the Raman conversion to S_{01} and S_{10} that at the highest pump energies of the circular polarized pump beam delivered by cavity A is of about 30% and few percent, respectively [Fig. 4(a)], gets few percent and 20%, respectively, with the beam delivered by cavity C [Fig. 4(c)]. The dependence upon ψ of the energy conversion to the Stokes lines is also substantially influenced by the pump beam optical properties: the conversion efficiency to S_{01} reduces to about 1% at $|\psi_{th}|=13°$ with the beam delivered by cavity A and at $|\psi_{th}|=30°$ with the highest divergence and beam quality factor radiation (C-cavity). It is worth mentioning that the energy conversion to S_{01} is no longer detectable at angles $|\psi|$ that are about 10% smaller than $|\psi_{th}|$. On the contrary, the conversion to S_{10} that increases as $|\psi|$ is reduced from 45° to $|\psi_{th}|$, is not influenced by the ellipticity of the pump radiation polarization as $|\psi|$ is reduced from $|\psi_{th}|$ to 0° (almost linear polarization).

The dependence of rotational Raman scattering upon the pump beam optical properties and $|\psi|$ is more clearly revealed by Fig. 5 (symbols), that shows the threshold pump
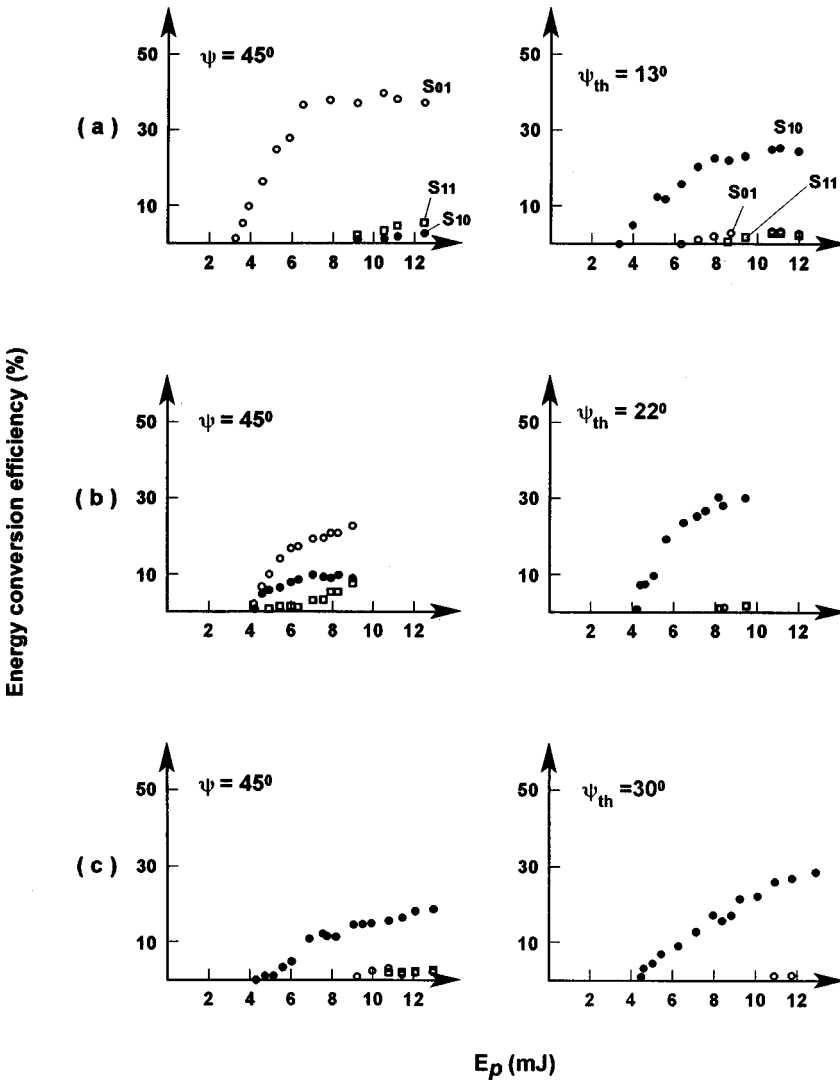

FIG. 4. Energy conversion efficiencies to rotational and vibrational lines for circular polarized radiation and for the elliptical polarized radiation providing, at highest pump energies, conversion efficiencies to S_{01} of about 1%, for the XeCl laser fitted with: (a) cavity A; (b) cavity B; (c) cavity C.
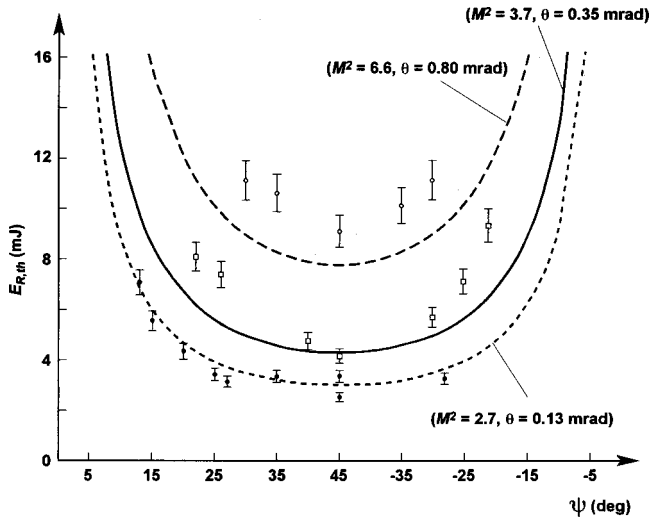
FIG. 5. Experimental threshold energies of the S_{01} line (symbols) versus the ellipticity angle for all tested laser beams. The energy conversion to S_{01} is not longer detectable at angles $|\psi|$ that are about 10% smaller than $|\psi_{th}|$. The lines show $E_{R,th}$ versus ψ obtained by Eq. (9) and the threshold condition $G = 24$.

energy for rotational scattering $E_{R,th}$ as a function of ψ, where $E_{R,th}$ represents the pump energy required to get 1% of energy conversion efficiency to S_{01}. One observes from Fig. 5 that the energy conversion to S_{01} is no longer detectable at angles $|\psi| < 13°$, $< 22°$, and $< 30°$ as the beam quality factor (divergence) is varied from $M^2 = 2.7$, 3.7, and $6.6(\theta = 0.13, 0.35, 0.8 \text{ mrad})$, respectively.

Ellipticity degree and optical properties of the pump radiation also influence the time evolution of vibrational and rotational Stokes pulses. Figure 6(a) and 6(b) show the temporal evolution of the S_{01} (solid line) and S_{10} pulse (dotted line) generated by using the circularly and elliptical polarized ($|\psi_{th}| = 13°$) laser radiation delivered by cavity A at a pump beam energy $E_p = 9$ mJ. We have used different oscilloscope vertical scales during the monitoring of the pulses in Fig. 6. One observes from Fig. 6(a) that the Raman conversion occurs nearly simultaneously to both lines, but the S_{10} pulse ends before the S_{01} pulse terminates. Then, the vibrational line pulse has a width of only 3 ns (FWHM), whereas the rotational line pulse is 8 ns long. On the contrary, one observes from Fig. 6(b) that the Raman conversion to S_{10} occurs $\sim$ 5 ns before the generation of the rotationally shifted S_{01} emission and lasts longer at $|\psi_{th}| = 13°$. The time evolutions of the Stokes pulses obtained with the pump beam having the highest M^2 and θ values (C cavity) are less dependent upon ψ. Figures 7(a) and 7(b) show the S_{01} (solid line) and S_{10} (dotted line) Stokes pulses monitored at $|\psi| = 45°$ and at $|\psi| = 35°$, respectively, for a pump beam energy of 7.5 mJ. One observes at first that the S_{01} emission is delayed of about 10 ns from the onset of the S_{10} line and lasts shorter at $|\psi| = 45°$, and secondly, that the rotational Stokes pulse width reduces with $|\psi|$.

IV. DISCUSSION AND CONCLUSION

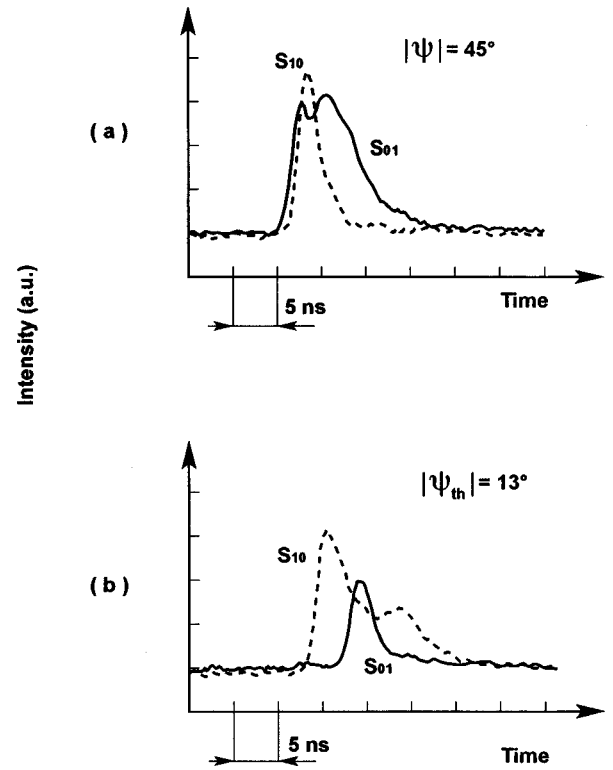The experimental results of Figs. 4–7 reveal that the dependence of SRRS upon ψ is affected by pump beam param-

FIG. 6. Time evolutions of the Stokes lines S_{01} (solid line) and S_{10} (dotted line) at $E_p = 9$ mJ for: (a) circular and (b) elliptical polarized radiation. The pulses have been monitored by using different oscilloscope vertical scales. The pump radiation was characterized by $M^2 = 2.7$ and $\theta = 0.13$ mrad.

eters. In particular, Fig. 5 shows the dependence of $E_{R,th}(\psi)$ upon M^2 and θ. Let us analytically retrieve $E_{R,th}(\psi)$ under steady-state conditions, being the dephasing time $(2\pi\Delta V)^{-1}$ much smaller than the pump pulse width ($\Delta t = 13$ ns) under our experimental conditions [8,20]. The comparison between the experimental and analytical dependence of $E_{R,th}$ upon ψ, may allow a better understanding of experimental results. Under steady-state conditions and for a focused multimode laser pulse with beam quality factor M^2, the Stokes power will grow as $\exp(G)$ where the cumulative gain coefficient G is given by [8,21]

$$G \cong [4g_R(E_p/(\Delta t M^2))\tan^{-1}(l/b)]/(\lambda_S + \lambda_p), \quad (9)$$

l is the length of the Raman cell, $b = 2\pi w_{po}^2/(\lambda_p M^2)$ is the confocal parameter, and w_{po} is the pump beam radius at the focus.

The onset of a steady-state threshold for stimulated scattering processes [22] is usually defined in terms of a threshold pump energy $E_{R,th}$ representing the energy at which the energy conversion efficiency to Stokes radiation reaches 1%. Following Laubereau and Kaiser [23], we take $G = 24$ as the appropriate condition, leading to a pump to S_{01}-Stokes' conversion efficiency of 1%. Then, the threshold energy of the S_{01} line $E_{R,th}(\psi)$, can be determined by introducing in Eq. (9) the parameters characterizing pump radiation, cell, and g_R that depends upon ψ. The results are shown in Fig. 5 as lines, whereas the experimental $E_{R,th}$ values are shown by
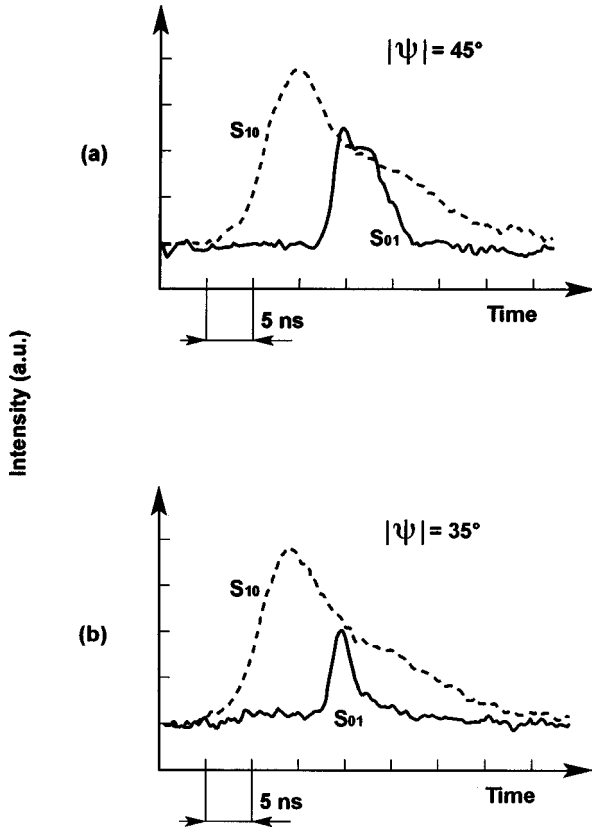
FIG. 7. Time evolutions of the Stokes lines S_{01} (solid line) and S_{10} (dotted line) at $E_p = 7.5$ mJ for (a) circular and (b) elliptical polarized radiation. The beam with $M^2 = 6.6$ and $\theta = 0.80$ mrad is used as pump. The pulses have been monitored by using different oscilloscope vertical scales.

symbols. One observes, from Fig. 5, a satisfactory accordance between theory and experimental data up to angles $|\psi| > 13°$, for the pump radiation with the lowest M^2 and θ values (dotted line). Whereas, the experimentally determined threshold energies get quite larger than theoretical values at angles $|\psi| < 25°$ for the laser beam with $M^2 = 3.7$ and $\theta = 0.35$ mrad (solid line). The experimental energy threshold values measured with the beam delivered by the C cavity ($M^2 = 6.6$ and $\theta = 0.8$ mrad) are instead quite larger than theoretical values at every ψ (dashed line).

Gain suppression effects on vibrational Raman scattering and their influence on the competition between rotational and vibrational scattering must be invoked to understand the differences between analytical and experimental data of Fig. 5. As has been mentioned, the vibrational gain is expected to be suppressed if the phase-matched angles of Stokes and anti-Stokes waves, $\varphi_S = 5.15$ and $\varphi_{AS} = 3.98$ mrad, respectively, are well contained within the diffraction angle δ propagating within the pump focal zone ($\delta \geq \varphi_S$). One gets from Table I that $\delta \cong 1.4 \varphi_S$ when the beam delivered by cavity A is focused in the Raman cell, whereas $\delta \cong 1.05 \varphi_S$ when the beam delivered by cavity C is used. Then, gain suppression effects on SVRS are expected to occur under all tested experimental conditions. As has been stated, the gain coefficient for the S_{10} vibrational line g_V, should reduce as a consequence of the Stokes-anti-Stokes coupling originating from the focus-

ing. Experimentally, this effect has most often been observed as increased Raman thresholds [8]. Hence, we can use the threshold condition for stimulated scattering processes to estimate the "effective vibrational Raman gain" that we indicate by $g_{V\text{-eff}}$. Following Laubereau and Kaiser [23] and in accord with the arguments presented above, we take

$$G \cong \{4 g_{V\text{eff}}[E_{V,th}/(\Delta t M^2)]\tan^{-1}(l/b)\}/(\lambda_V + \lambda_p) = 24 \tag{10}$$

as the appropriate condition leading to a pump to S_{10}-Stokes' conversion efficiency of 1%, where $E_{V,th}$ is the pump energy required to get 1% of energy conversion efficiency to S_{10} of wavelength λ_V. The threshold pump energy values $E_{V,th}$ needed to retrieve $g_{V\text{-eff}}$ by Eq. (10), may be retrieved by the energy conversion efficiency measurements to S_{10} obtained with the elliptical polarized pump radiation providing conversion efficiencies to $S_{01} \lesssim 1\%$, at the highest pump energies. As has been mentioned, we found with linearly polarized pump radiation (rotational scattering is no longer detectable) that the S_{10}-line threshold energy $E_{V,th}$ was equal to that obtained at $\psi \cong \psi_{th}$. One gets from Fig. 4(a) that the threshold pump energy of the S_{10}-Stokes line is $E_{V,th} = (3.3 \pm 0.3)$ mJ at $\psi_{th} = 13°$, when the beam delivered by cavity A is used. Whereas, one gets $E_{V,th} = (4.2 \pm 0.4)$ mJ at $\psi_{th} = 22°$, and $E_{V,th} = (4.4 \pm 0.4)$ mJ at $\psi_{th} = 30°$, when the beams delivered by the B [Fig. 4(b)] and C cavity [Fig. 4(c)] are used, respectively. The "effective vibrational Raman gain" $g_{V\text{-eff}}$ can then be determined by introducing in Eq. (10) experimental energy threshold values and pump radiation, and cell parameters. The $g_{V\text{-eff}}$ values obtained are reported on Table I, besides the corresponding $E_{V\text{-th}}$ values and are shown on Fig. 1 as dashed/dotted lines. One observes from Table I that the vibrational Raman gain $g_V = 7.6 \times 10^{-9}$ cm/W is reduced of $\sim 65\%$ as a consequence of gain suppression effects, when the beam delivered by cavity A ($M^2 = 2.7$, $\theta = 0.13$ mrad) is used to excite the Raman medium, whereas a gain reduction lower than 30% is observed with the beam characterized by $M^2 = 6.6$ and $\theta = 0.8$ mrad. Figure 8 shows $g_{V\text{-eff}}$ versus δ (dots) and one observes in accord with the arguments presented above, that the vibrational Raman gain reduces fast for diffraction angles $\delta > \varphi_S = 5.15$ mrad. In particular, the vibrational gain reduces of 30% when $\delta \cong 1.05 \varphi_S$ and of about 65% when $\delta \cong 1.4 \varphi_S$.

Let us use the "effective vibrational gain" value $g_{V\text{-eff}} = 2.7 \times 10^{-9}$ cm/W to support at first the experimental results obtained with the pump beam delivered by cavity A. Figure 1 reveals that $g_{V\text{-eff}} \cong 0.9 g_R$ when the circular polarized pump radiation is used, and as a consequence, rotational scattering is favored with respect to vibrational scattering [Fig. 3(a)] and higher conversion efficiencies to S_{01} are measured. Indeed, the Raman conversion to S_{01} and S_{10} is of about 30% and few percent, respectively, at the highest pump energies. As has been stated Fig. 6(a) shows that the Raman conversion to rotational and vibrational lines occurs nearly simultaneously at $E_p = 9$ mJ but, the S_{10} pulse ends before the S_{01} pulse terminates. We believe that the fast termination of the S_{10} pulse is due to the Stokes amplitude reduction with z until condition (2) is approached, which occurs in the limit of
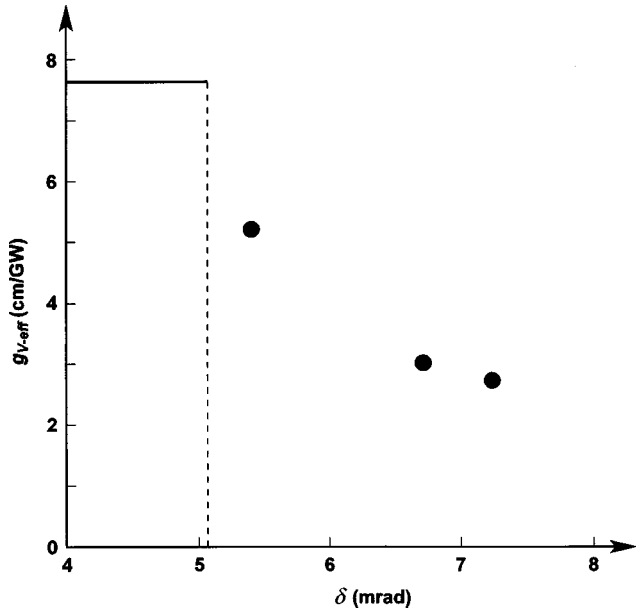
FIG. 8. Effective vibrational Raman gain (dots) versus the diffraction angle δ. The solid line shows the g_V value. The dashed line has been drawn at $\delta = 5.15$ mrad.

perfect phase matching. Then, we believe that the time evolution of the S_{10} pulse shown in Fig. 6(a) is a clear experimental evidence of gain suppression effects on SVRS, which may be observed when the vibrational gain is significantly reduced by gain suppression, as it happens under our experimental conditions.

Figure 1 shows that the ratio g_V/g_R increases with the ellipticity degree of the pump radiation and one gets that $g_{V\text{-eff}} \cong 2.2 g_R$ at $\psi_{th} = 13°$ with the laser beam delivered by cavity A. Then, vibrational scattering is more favored than rotational scattering at $\psi_{th} = 13°$, and as a consequences the conversion efficiency to S_{10} is significantly larger than that to S_{01} [Fig. 4(a)] and the Raman conversion to S_{10} occurs ~5 ns before the generation of S_{01} and lasts longer at $E_p = 9$ mJ [Fig. 6(b)]. Hence, rotational scattering is more favored when gain suppression effects on SVRS make the effective vibrational Raman gain lower than g_R. This conclusion is further supported by the experimental results of Figs. 4–7. Figures 4(c) and 5 (open dots) show that the energy conversion efficiencies to S_{01} are quite low ($1-2\%$) and that

the threshold energies are significantly larger than theoretical values (dashed line) when the beam delivered by cavity C is focused in the Raman medium. In fact, Fig. 1 reveals that $g_{V\text{-eff}} \geq 1.8 g_R$ at every ψ value when the beam delivered by cavity C is used. Thus, the vibrational scattering is more efficient for the high value of the "effective vibrational gain" with respect to the rotational gain value. The vibrational gain is less affected by gain suppression effects when the beam delivered by cavity C is used, since the value of diffraction angle δ is quite close to that of the phase matching angle φ_S (Table I). Figure 4(b) also reveals that the Raman conversion to S_{01} that was of about 22% at $\psi = 45°$ and $E_p = 9$ mJ, reduces to about 1% at $\psi_{th} = 22°$, as the ratio $g_{V\text{-eff}}/g_R$ increases from about 1 to about 1.5.

In conclusion, it has been show that the Raman conversion to rotational Stokes lines by elliptical polarized laser radiation is quite dependent on the "effective vibrational Raman gain," which in turn depends on the optical beam parameters M^2 and θ, as well as on the focal length of the focusing lens. The cumulative gain coefficient G and the threshold condition $G = 24$, have been used to compute the "effective vibrational Raman gain" $g_{V\text{-eff}}$ and evaluate the dependence of gain suppression effects on SVRS upon the ratio δ/φ_S. It has been found that the vibrational Raman gain reduces fast as the diffraction angle δ gets larger than the phase matching angle φ_S. Indeed, g_V reduced of 30% for $\delta \cong 1.05 \varphi_S$ and of about 65% for $\delta \cong 1.4 \varphi_S$. It has then, been found that rotational Raman scattering is more favored than vibrational scattering when $g_{V\text{-eff}} < g_R$ but, the energy conversion efficiency to rotational Stokes radiation reduces to few percent when $g_{V\text{-eff}} \geq 1.5 g_R$ as it is revealed by Figs. 3–7. So, a good understanding of theory and experiments has been provided in this paper and the conditions that maximise SRRS have clearly been defined.

Finally, it has been shown in this paper, that the experimental evidence of gain suppression effects on SVRS may take the form of a fast termination of the S_{10} pulse [Fig. 6(a)], accordingly to Eq. (2).

We believe that the experimental results reported in this paper can be of support in view of extending the tuning range of laser sources by means of the stimulated Raman scattering technique since simple rules that allow maximizing the Raman conversion to rotational or vibrational lines have been derived.

[1] G. Eckhardt, R. W. Hellwarth, F. J. McClung, S. E. Schwarz, D. Weiner, and E. J. Woodbury, Phys. Rev. Lett. **9**, 455 (1962).

[2] V. S. Averbakh, A. I. Makarov, and V. I. Talanov, Kvant. Electron. (Moscow) **5**, 2207 (1975) [Sov. J. Quantum Electron. **8**, 472 (1978)].

[3] V. Krylov, A. Rebane, O. Ollikainen, D. Erni, U. Wild, V. Bespalov, and D. Staselko, Opt. Lett. **21**, 381 (1996).

[4] T. Pritchett, J. Smith, G. McIntyre, T. R. Moore, and B. G. Oldaker, J. Mod. Opt. **46**, 949 (1999).

[5] Y. Irie and T. Imasaka, Opt. Lett. **20**, 2072 (1995).

[6] S. Wada, H. Tashiro, Y. Urata, L. Thi Thi, A. Kasai, and K. Toyoda, Appl. Phys. B: Lasers Opt. **57**, 435 (1993).

[7] F. Hanson and P. Poirier, IEEE J. Quantum Electron. **29**, 2342 (1993).

[8] M. R. Perrone, V. Piccinno, G. De Nunzio, and V. Nassisi, IEEE J. Quantum Electron. **33**, 938 (1997).

[9] D. Diso, M. R. Perrone, and L. Protopapa, Appl. Phys. B: Lasers Opt. **70**, 529 (2000).

[10] Y. R. Shen and N. Bloembergen, Phys. Rev. **137**, A1787 (1965).

[11] M. D. Duncan, R. Mahon, J. Reintjes, and L. L. Tankersley, Opt. Lett. **11**, 803 (1986).

[12] Y. R. Shen and N. Bloembergen, Phys. Rev. Lett. **12**, 504 (1964).

[13] Landolt and Bornstein, *Zahlenwarte und Functionen aus Physik, Chemie, Astronomie, Geophysik und Technik*, Landolt-Bornstein, New Series, Vol. II, Pt. 8 (Springer-Verlag, Berlin, 1962).

[14] D. Wright, P. Greve, J. Fleischer, and L. Austin, Opt. Quantum Electron. **24**, S993 (1992).

[15] G. V. Venkin, Y. A. Il'inskii, and G. M. Mikheev, Kvant. Elektron. (Moscow) **12**, 608 (1985) [Sov. J. Quantum Electron. **15**, 395 (1985)].

[16] R. W. Carlson and W. R. Fenner, Astrophys. J. **178**, 551 (1972).

[17] W. Bischel and G. Black, in *Excimer Lasers* 1983, edited by C. K. Rhodes, H. Egger, and H. Pummer, AIP Conf. Proc. No. **100** (AIP, New York, 1983).

[18] C. Giuri, M. R. Perrone, D. Flori, A. Piegari, and S. Scaglione, Appl. Phys. Lett. **65**, 655 (1994).

[19] M. R. Perrone, V. Piccinno, and G. De Nunzio, Appl. Phys. B: Lasers Opt. **65**, 569 (1997).

[20] M. G. Raymer, J. Mostowski, and J. L. Carlsten, Phys. Rev. A **19**, 2304 (1979).

[21] J. Carlsten and R. G. Wenzel, IEEE J. Quantum Electron. **QE-19**, 1407 (1983).

[22] S. Kawasaki, T. Imasaka, and N. Ishibashi, Appl. Phys. B: Lasers Opt. **52**, 211 (1991).

[23] A. Laubereau and W. Kaiser, Rev. Mod. Phys. **50**, 607 (1978).